

# Crystal structure and luminescence properties of 4-(4-benzoyloxy-2-hydroxyphenyl)-2,2-difluoro-6-phenyl-1,3,2-dioxaborine

B. V. Bukvetskii, E. V. Fedorenko,\* and A. G. Mirochnik

Institute of Chemistry, Far East Branch of the Russian Academy of Sciences,  
159 prosp. 100-letiya Vladivostoka, 690022 Vladivostok, Russian Federation.  
Fax: +7 (423 2) 31 1889. E-mail: gev@ich.dvo.ru

The crystal structure of 4-(4-benzoyloxy-2-hydroxyphenyl)-2,2-difluoro-6-phenyl-1,3,2-dioxaborine (**1**) was determined by X-ray diffraction analysis.  $\pi$ - $\pi$ -Stacking interaction between the molecules results in joining the molecules into a three-dimensional layered framework. Luminescence of the aggregates is observed in concentrated solutions of compound **1**. Two routes of excimer formation in crystal were revealed by steady-state and time-resolved luminescence spectroscopy: *via* excitation of single molecules and *via* excitation of aggregates.

**Key words:** boron difluoride  $\beta$ -diketonates, crystal structure, stacking factor, excimer.

Boron difluoride  $\beta$ -diketonates have first been synthesized at the beginning of the XX century.<sup>1</sup> Increasing interest in this class of compounds is observed<sup>2–4</sup> presently due to a permanent extension of the sphere of their application as laser dyes,<sup>5</sup> active components of solar collectors,<sup>6</sup> photosensitive components of materials for electrophotography,<sup>7,8</sup> materials for nonlinear optics,<sup>9</sup> and organic photodiodes.<sup>10</sup> Therefore, investigation of the spectral luminescence properties of boron difluoride  $\beta$ -diketonates is an urgent task.

We have previously shown that the introduction of the methyl substituent into the phenyl ring of boron difluoride benzoylacetates<sup>11</sup> and dibenzoylmethanates<sup>12</sup> substantially changes the crystal packing and, as a consequence, the luminescence properties of the crystals. In continuation of these works, we studied the interrelation between the crystal structure and luminescence properties of 4-(4-benzoyloxy-2-hydroxyphenyl)-2,2-difluoro-6-phenyl-1,3,2-dioxaborine (**1**), *viz.*, dibenzoylmethanate bearing the bulky substituent (oxybenzoic group) in the *para*-position. The spectral luminescence properties of solutions with different concentrations and crystals of compound **1** were studied in comparison. The study of the luminescence properties of compounds with a high luminophore content is of special interest, since this class of compounds is characterized by the formation of excimers,<sup>13–15</sup> resulting in the enhancement of photostability of boron difluoride  $\beta$ -diketonates in the polymer matrix and an increase in the luminescence intensity of the related polymer compositions under UV irradiation.<sup>16,17</sup>

## Experimental

**1-(4-Benzoyloxy-2-hydroxyphenyl)-3-phenylpropane-1,3-dione** was synthesized similarly to *o*-hydroxydibenzoylmethane using a known procedure<sup>18</sup> in two stages.

(1) A mixture of 2,4-dihydroxyacetophenone (15.2 g), benzoyl chloride (35 g), and pyridine (30 mL) was heated in a water bath for 30 min. Then 10% hydrochloric acid (100 mL) was added to the reaction mixture. The product was extracted with ethyl acetate, and ethyl acetate was distilled on a rotary evaporator. 2,4-Dibenzoyloxyacetophenone that formed was recrystallized from isopropyl alcohol. The yield was 22.32 g (62.0%). Found (%): C, 73.27; H, 4.38. C<sub>22</sub>H<sub>16</sub>O<sub>5</sub>. Calculated (%): C, 73.33; H, 4.48. IR (KBr),  $\nu$ /cm<sup>-1</sup>: 1743 (O—C=O), 1688 (CH<sub>3</sub>C=O), 1600 (C<sub>6</sub>H<sub>5</sub>), 1244 (—O—CO).

(2) A solution of 2,4-dibenzoyloxyacetophenone (20 g) in pyridine (30 mL) was heated to 50 °C, and powdered potassium hydroxide (5.5 g) heated to 80 °C was added with stirring. The mixture was stirred for 30 min at 50 °C, and 1-(4-benzoyloxy-2-hydroxyphenyl)-3-phenylpropane-1,3-dione precipitated. After cooling, the pasty reaction mixture was dissolved in 10% acetic acid (100 mL). The precipitate was filtered off, washed with water, and recrystallized from isopropyl alcohol. The yield was 15.42 g (77.1%). Found (%): C, 73.47; H, 4.56. C<sub>22</sub>H<sub>16</sub>O<sub>5</sub>. Calculated (%): C, 73.33; H, 4.48. IR (KBr),  $\nu$ /cm<sup>-1</sup>: 3700 (O—H), 3604 (O—H $\cdots$ O), 1743 (O—C=O), 1629 (C=O), 1600 (C<sub>6</sub>H<sub>5</sub>), 1589 (C=CH—CO).

**4-(4-Benzoyloxy-2-hydroxyphenyl)-2,2-difluoro-6-phenyl-1,3,2-dioxaborine (1).** A mixture of 1-(4-benzoyloxy-2-hydroxyphenyl)-3-phenylpropane-1,3-dione (2.4 g) and boron trifluoride etherate (1.9 mL) in toluene (20 mL) was refluxed for 5 min. The precipitate formed was filtered off, dried in air, and recrystallized from acetonitrile. The yield was 0.64 g (23.70%), m.p. 145–146 °C. Found (%): C, 64.82; H, 3.58. C<sub>22</sub>H<sub>15</sub>BF<sub>2</sub>O<sub>5</sub>.

Calculated (%): C, 64.74; H, 3.70. IR (KBr),  $\nu/\text{cm}^{-1}$ : 3196 (O—H...O); 1741 (O=C=O); 1598 (C<sub>6</sub>H<sub>5</sub>); 1531 (C=CH—CO); 1141, 1107 (B—O); 1043, 1022 (B—F).

Absorption spectra were recorded on a Shimadzu UV-2550 spectrometer in 10-mm cells and between quartz glasses at a concentration of  $6 \cdot 10^{-3} \text{ mol L}^{-1}$ . Excitation and luminescence spectra were detected on a Shimadzu RF5301 instrument in cells of 10 and 2 mm thick at the standard arrangement of the sample, in a 1-mm cell, and between quartz glasses at the frontal arrangement of the sample. The luminescence decay kinetics was measured on a FluoTime 200 laser picosecond spectrofluorimeter (PicoQuant) ( $\lambda_{\text{ex}} = 370 \text{ nm}$ ). The frontal arrangement of the sample was used for a solution ( $C = 10^{-3} \text{ mol L}^{-1}$ ) and powder of compound **1**. IR spectra were recorded on an IRAffinity-1 Shimadzu spectrometer.

**X-ray diffraction analysis of compound 1.** The full X-ray diffraction study of yellow-colored compound **1** was performed on a SMART-1000 CCD diffractometer (Bruker) at 296(2) K using Mo-K $\alpha$  radiation. Experimental data from the sample were collected by three groups (906 frames each) at the angles  $\varphi = 0.90$  and  $180^\circ$  in the  $\varphi$  scan mode with an increment of  $0.2^\circ$  and an exposure of 20 s per each frame. The unit cell parameters were refined and the integral intensities were recalculated to structur-

**Table 1.** Crystallographic data and details of X-ray diffraction experiment for compound **1**

Parameter	<b>1</b>
Empirical formula	C <sub>22</sub> H <sub>15</sub> BF <sub>2</sub> O <sub>5</sub>
<i>T</i> /K	296
Molecular weight	408.15
Space group	<i>P</i> $\bar{1}$
<i>a</i> /Å	7.460(2)
<i>b</i> /Å	9.446(2)
<i>c</i> /Å	14.223(3)
$\alpha$ /deg	73.656(4)
$\beta$ /deg	87.805(4)
$\gamma$ /deg	74.706(4)
<i>Z</i>	2
$d_{\text{calc}}/\text{g cm}^{-3}$	1.462
$\mu/\text{mm}^{-1}$	0.115
F(000)	420
Crystal size/mm	0.30×0.20×0.13
$\theta$ range of data collection/deg	2.33–25.10
Ranges of reflection indices	$-8 \leq h \leq 8, -11 \leq k \leq 11,$ $-16 \leq l \leq 16$
Measured reflections	9476
Independent reflections	3292
$R_{\text{int}}$	0.0347
Completeness for $\theta = 25.10^\circ$ (%)	99.6
Number of reflections with $I > 2\sigma(I)$	1844
Number of refinement variables	276
Googness-of-fit	0.988
<i>R</i> -factors for $I > 2\sigma(I)$ :	
$R_1$	0.0427
$wR_2$	0.866
Extinction coefficients	0.0057(9)
Residual electron density (min/max)/e Å <sup>-3</sup>	-0.305/0.331

**Table 2.** Selected bond lengths (*d*) and bond angles ( $\omega$ ) in compound **1**

Bond	<i>d</i> /Å	Angle	$\omega$ /deg
B—F(2)	1.335(3)	F(2)—B—F(1)	111.9(2)
B—F(1)	1.359(3)	C(1)—O(1)—B	124.0(2)
B—O(2)	1.463(3)	C(3)—O(2)—B	123.9(2)
B—O(1)	1.485(3)	O(1)—C(1)—C(2)	119.2(2)
O(1)—C(1)	1.314(2)	C(3)—C(2)—C(1)	121.3(2)
O(2)—C(3)	1.307(2)	O(2)—C(3)—C(2)	120.5(2)
O(3)—C(22)	1.354(2)	O(2)—C(3)—C(11)	114.6(2)
O(3)—H(3)	0.94(3)	O(1)—C(1)—C(21)	115.1(2)
C(1)—C(2)	1.381(3)		
C(1)—C(21)	1.458(3)		
C(2)—C(3)	1.374(3)		
C(3)—C(11)	1.434(3)		

al amplitude module using the SMART program package.<sup>19</sup> The structure was determined by a direct method followed by the refinement of positional and thermal parameters in the anisotropic approximation for all non-hydrogen atoms using the SHELXTL PLUS program package.<sup>20</sup> The position of the H(3) hydrogen atom of the OH group was obtained from the electron density distribution synthesis in the cell and refined as an independent one without bond restraint. The positions of other hydrogen atoms were revealed from the electron density syntheses but gave no basic novelty. The calculated and refined by the riding model positions with the C—H distance equal to 0.93 Å were used for the further work.

The main crystallographic parameters of the studied samples, characteristics of the X-ray diffraction experiment, and refinement details of the structure model using least squares are presented in Table 1. Interatomic spacings and bond angles are given in Table 2. The structure of molecule **1** and the arrangement of adjacent molecules in stacks are shown in Fig. 1.

The crystallographic information was deposited with the Cambridge Crystallographic Data Centre (CCDC 910951) and is available at [www.ccdc.cam.ac.uk/data\\_request/cif](http://www.ccdc.cam.ac.uk/data_request/cif).

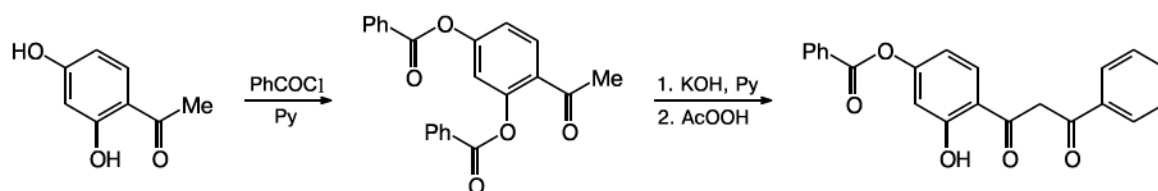
## Results and Discussion

The ligand for the synthesis of complex **1** was obtained by the acylation of 2,4-dihydroxyacetophenone followed by the Baker—Venkataraman rearrangement (Scheme 1). Under the synthesis conditions (potassium hydroxide in pyridine), only the above rearrangement is observed and, contrary to expectations, the benzoyl group in the *para*-position of 2,4-benzoyloxyacetophenone is not removed even in a fourfold excess of alkali. Thus, 2,4-dihydroxydibenzoylmethanes with the protected hydroxy group in the *para*-position can be obtained *via* the presented scheme.

The synthesized  $\beta$ -diketone is readily chelated by boron trifluoride etherate (Scheme 2). Compound **1** represents yellow crystals with green luminescence.

The structure of compound **1** is built of isolated, predominantly planar molecules similarly to molecules of boron benzoylacetate difluoride and its analogs.<sup>11–13</sup>

Scheme 1



$\pi$ - $\pi$ -Stacking interactions between the molecules result in joining the molecules into a three-dimensional framework.

The peculiarities of the structure formation are presented in Fig. 1.

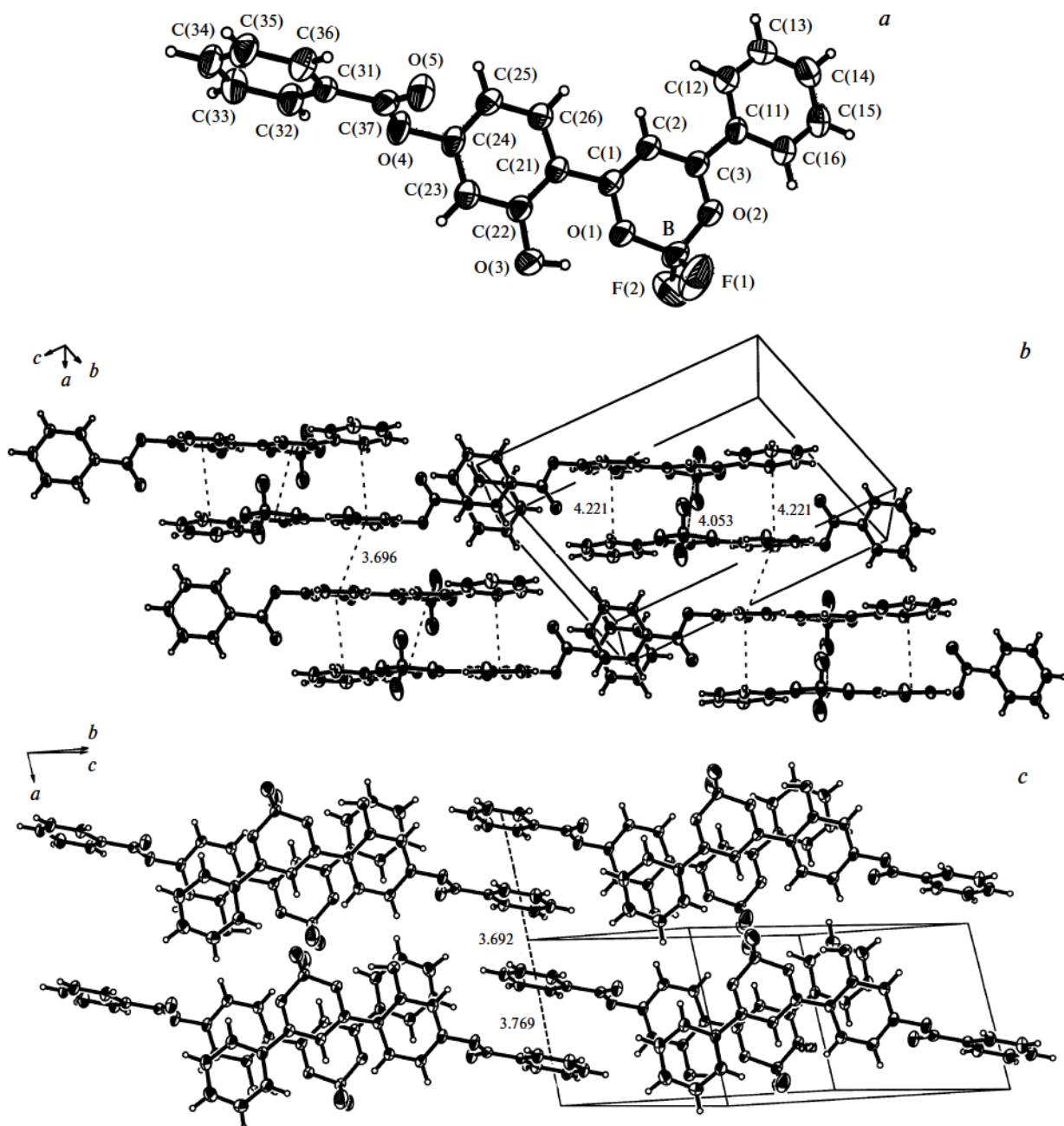
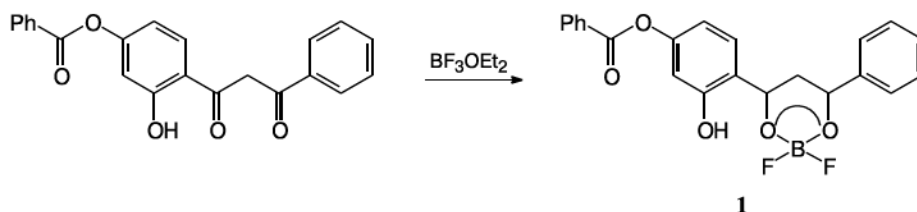


Fig. 1. General crystal structure of molecule 1 (a), the crystal structure with spacings between centroids of overlapped fields (b), and the fragment of the unfolded layer (c) in crystal structure 1 with the  $\pi$ - $\pi$ -stacking interaction between the benzoyl groups.

Scheme 2



The chelate ring in molecule **1** and phenyl rings linked to it lie nearly in one plane, and the benzoyl group is arranged at an angle of  $76^\circ$  to this plane (see Fig. 1). The C—C bonds of the chelate are close to sesquialteral ( $d = 1.38 \text{ \AA}$ ), indicating an efficient  $\pi$ — $\pi$ -conjugation and symmetrical electron density distribution in the diketonate cycle, unlike other boron difluoride dibenzoylmethanates with different substituents in the phenyl rings where the C—C bonds of the chelate are nonsymmetrical.<sup>21,22</sup> The ordinary C—C bonds in compound **1** between the chelate and phenyl rings are shortened (C(21)—C(1)  $1.458 \text{ \AA}$ , C(3)—C(11)  $1.464 \text{ \AA}$ ), indicating the  $\pi$ — $\pi$ -conjugation between the chelate and phenyl rings. The  $\pi$ — $\pi$ -conjugation in molecule **1** is stronger than that in boron difluoride dibenzoylmethanate<sup>13,22</sup> (ordinary bond  $1.474 \text{ \AA}$ ) and comparable with the  $\pi$ — $\pi$ -conjugation in boron difluoride dibenzoylmethanate having different substituents in the phenyl rings<sup>21,22</sup> ( $1.45$ – $1.46 \text{ \AA}$ ). The hydroxy group in compound **1** is bound through the intramolecular hydrogen bond to the oxygen atom of the chelate (O(3)—H(3)···O(1),  $d(\text{O}(3)\text{—O}(1)) = 2.553(2) \text{ \AA}$ ,  $d(\text{O}(3)\text{—H}(3)) = 0.94(3) \text{ \AA}$ ,  $d(\text{H}(3)\text{—O}(1)) = 1.71(3) \text{ \AA}$ ,  $\angle \text{O}(3)\text{—H}(3)\text{—O}(1) = 148(1)^\circ$ ). The C(1)—O(1) and C(1)—B bonds are elongated compared to the symmetrical C—O and C—B bonds of the chelate ring due to the action of the hydrogen bond on the O(1) atom from the hydroxy group:  $d(\text{C}(1)\text{—O}(1)) = 1.314(2)$  and  $d(\text{O}(1)\text{—B}) = 1.485(3) \text{ \AA}$  compared to  $d(\text{C}(3)\text{—O}(2)) = 1.307(2)$  and  $d(\text{O}(2)\text{—B}) = 1.463(3) \text{ \AA}$ , respectively.

Molecules **1** multiplied by symmetry centers and translations along the crystallographic axis  $b$  are arranged in stacks of oriented rigidly parallel molecules. The action of the symmetry center of the type  $(0.5, 0.5, 0.5)$  results in the paired (in direction  $[012]$ ) arrangement of adjacent molecules above each other with unfolding by  $180^\circ$  and a distance between the planes of  $3.668 \text{ \AA}$ . This arrangement of the molecules is accompanied by the  $\pi$ — $\pi$ -stacking interaction between both chelate and phenyl rings of these molecules with the distances between the centroids equal to  $4.053$  and  $4.221 \text{ \AA}$ , respectively (see Fig. 1,  $b$ ). These pairs of molecules are reflected in the symmetry center of the  $(0.5, 0, 0.5)$  type and packed in infinite and somewhat skewed in the direction of the crystallographic axis  $c$  stacks by the formation of the  $\pi$ — $\pi$ -stacking interaction between the phenyl rings from the attached benzoyl groups of the

molecules. The distance between the planes of the phenyl ring C(21)—C(26) and its reflection in the symmetry center C(21)'—C(26)' in the site of their overlapping is  $3.410 \text{ \AA}$  at the distance between their centroids equal to  $3.696 \text{ \AA}$  (see Fig. 1,  $b$ ).

A peculiarity of the formation of the crystal structure of compound **1** is the fact that the benzoyl groups arranged at an angle of  $76^\circ$  to the major plane of the molecule and multiplied in the direction of the crystallographic axis  $a$  by the symmetry centers  $(0, 0, 0)$  and  $(0.5, 0, 0)$  form an infinite stack of parallel phenyl rings with the  $\pi$ — $\pi$ -stacking interaction between them. The parameters of this interaction provide distances between the centroids in the sites of overlapping of  $3.432 \text{ \AA}$  and  $3.492 \text{ \AA}$  between the phenyl ring planes C(31)—C(36) multiplied by the method indicated above at two crystallographically independent distances of  $3.692$  and  $3.769 \text{ \AA}$ , respectively (see Fig. 1,  $c$ ). This peculiarity of structure formation represents infinite layers of paired molecules **1** parallel to the plane  $(011)$  (see Fig. 1,  $b$ ). The three-dimensional framework of structure **1** can conveniently be presented by the conjugation of these layers by the  $\pi$ — $\pi$ -stacking interaction between the C(21)—C(26) phenyl rings and their reflection in the symmetry centers.

Crystals **1** have an intense green luminescence, unlike the aquamarine luminescence of solutions of compound **1** in organic solvents. The luminescence spectrum of the crystals exhibits a bathochromic shift relatively to the spectrum of the solution (for the crystals,  $\lambda_{\text{max}} = 535 \text{ nm}$ ; for the solutions at  $C = 10^{-5}$ – $10^{-4} \text{ mol L}^{-1}$ ,  $\lambda_{\text{max}} = 470 \text{ nm}$ ). This noticeable shift of the luminescence band maximum on going from the solution to crystals is caused, most likely, by different natures of the luminescence centers in solutions and in crystals. To elucidate the nature of the luminescence centers, we studied the excitation and luminescence spectra of crystals and solutions of compound **1** in acetonitrile at different concentrations (Figs 2, 3).

Monomeric luminescence with  $\lambda_{\text{max}} = 470 \text{ nm}$  obeying the Bouguer—Lambert—Beer law is observed for solutions with the concentration  $10^{-5} \text{ mol L}^{-1}$  and lower. The luminescence decay kinetics is monoexponential ( $\tau = 0.93 \text{ ns}$ ). For monomeric luminescence, the excitation spectrum almost coincides with the absorption spectrum (see Fig. 2). As it should be expected, luminescence quenching is observed when the concentration of the solu-

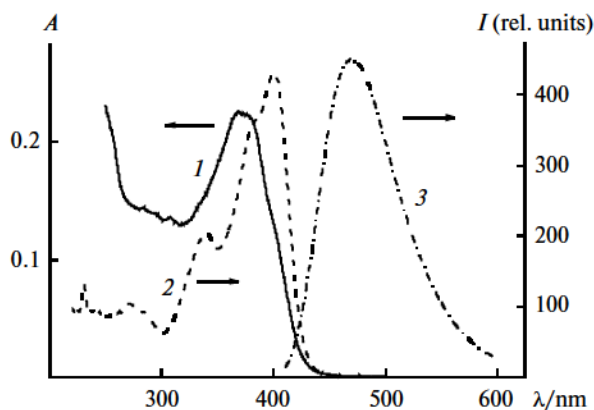


Fig. 2. Absorption (1), excitation (2), and luminescence (3) spectra of solutions of compound **1** in acetonitrile ( $C = 10^{-5} \text{ mol L}^{-1}$ ).

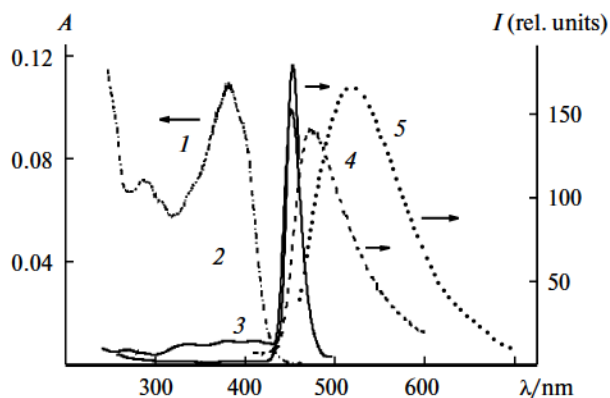


Fig. 3. Normalized absorption spectra (1), excitation spectra at  $\lambda_{\text{reg}} = 470$  (2) and  $520 \text{ nm}$  (3), and luminescence spectra at  $\lambda_{\text{ex}} = 370$  (4) and  $450 \text{ nm}$  (5) of a solution of compound **1** in acetonitrile ( $C = 0.006 \text{ mol L}^{-1}$ ) at the perpendicular arrangement of the cell.

tion increases: the integral luminescence intensity ( $\lambda_{\text{max}} = 470 \text{ nm}$ ) decreases by 30 times as the concentration changes from  $C = 5 \cdot 10^{-5}$  to  $10^{-3} \text{ mol L}^{-1}$  and excitation is carried out at the absorption maximum with  $\lambda_{\text{ex}} = 383 \text{ nm}$  (Fig. 4). In this case, the excitation spectrum exhibits only low-intensity bands in a region of  $370\text{--}400 \text{ nm}$  and an intense narrow band with a maximum at  $450 \text{ nm}$  (see Fig. 3). It was found that the change in the exciting wavelength by  $450 \text{ nm}$  results in a twofold decrease in the luminescence intensity of the concentrated solution compared to that of a dilute solution ( $10^{-5} \text{ mol L}^{-1}$ ), but the bathochromic shift of the luminescence band maximum ( $\lambda_{\text{max}} = 520 \text{ nm}$ ) (see Fig. 4). The dependence of the efficiency of the concentration quenching on the exciting wavelength was explained<sup>23</sup> by the formation of intermolecular aggregates excited by a wavelength different from the wavelength of the absorption band maximum of single molecules.

In fact, when the concentration increases to  $5 \cdot 10^{-4} \text{ mol L}^{-1}$ , the excitation spectrum is transformed

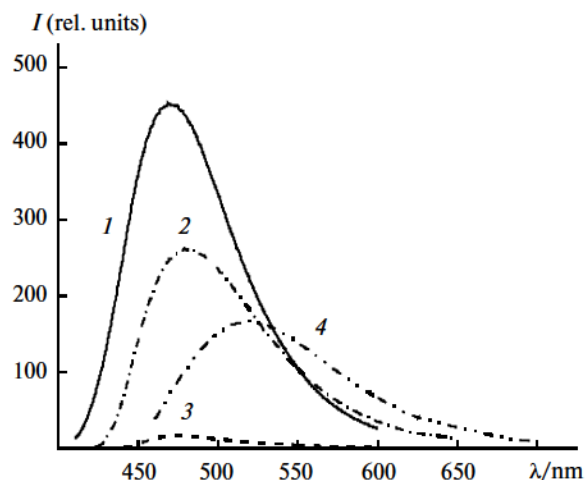


Fig. 4. Concentration quenching of luminescence of solutions of compound **1** in acetonitrile at concentrations of  $10^{-5}$  (1),  $5 \cdot 10^{-4}$  (2), and  $0.006 \text{ mol L}^{-1}$  ( $\lambda_{\text{ex}} = 370 \text{ nm}$ ) (3);  $0.006 \text{ mol L}^{-1}$  ( $\lambda_{\text{ex}} = 450 \text{ nm}$ ) (4).

into a narrow band with a maximum at  $430 \text{ nm}$ , which undergoes the bathochromic shift to  $450 \text{ nm}$  with the further increase in the concentration to  $6 \cdot 10^{-3} \text{ mol L}^{-1}$  (the measurements were carried out in a Shimadzu cell for concentrated solutions). The observed evolution of the excitation spectra with an increase in the concentration of compound **1** in solution (transformation of the spectrum into a narrow band bathochromically shifting relatively to the spectrum of the monomers and the bathochromic shift of the maximum with an increase in the concentration) is similar to the changes that occur in the absorption and luminescence excitation spectra of the J-aggregates.<sup>24–26</sup> In the absorption spectra of compound **1**, unlike solutions of polymethine dyes, no considerable changes are observed with concentrating (see Figs 2 and 3).

The decrease in the luminescence intensity of single molecules at high concentrations in solution can be due to the internal filter effect or to the formation of molecular aggregates. When studying the nature of concentration quenching of the luminescence of the rhodamine dyes, it was mentioned<sup>27</sup> that the deformation of the electronic absorption spectra upon association depends substantially on the force of the intermolecular interaction in the associate and the general spectrum remains almost unchanged at low degrees of association. In the case of compound **1**, the changes in the excitation and luminescence spectra with an increase in the concentration that are not accompanied by the deformation of the absorption spectra can be related to both the formation of weakly bound associates similar to those described earlier<sup>27</sup> and to the internal filter effect for monomeric luminescence with a simultaneous increase in the number of new luminescence centers excited by another wavelength. The spectral luminescence properties of concentrated solutions of compound **1** were

studied in detail to reveal the nature of the long-wavelength luminescence observed in these solutions.

A thin cell and frontal arrangement of the sample are usually used for spectra recording in the studies of the luminescence properties of the samples with a high absorbance ( $C = 5 \cdot 10^{-4} - 6 \cdot 10^{-3} \text{ mol L}^{-1}$ ). The study of the luminescence properties of a concentrated solution of compound **1** ( $6 \cdot 10^{-3} \text{ mol L}^{-1}$ ) in thin films between quartz glasses at the frontal arrangement of the sample showed that the absorption spectra and the excitation and luminescence spectra correspond to the spectra recorded for a dilute solution. Therefore, the decrease in the intensity of the monomeric luminescence band with an increase in the concentration of compound **1** is mainly associated with the internal filter effect. When only the internal filter effect acts, an increase in the absorbance should result in a smooth decrease in the excitation spectra intensity and its shift to the hypsochromic region.<sup>28</sup> The luminescence intensity remains unchanged for the complete light absorption at all wavelengths (the excitation spectra should represent a straight line).<sup>29</sup> In this case, the position of the luminescence maximum should not depend on the exciting wavelength. However, in our case, an increase in the optical path length, which was attained by using the cell with a thickness of 0.1 cm at the frontal arrangement of the sample, results in the long-wavelength shift of the excitation and luminescence spectra (Fig. 5). The monomeric luminescence bands in the excitation spectra disappear and only a narrow intense band at  $\lambda_{\text{max}} = 450 \text{ nm}$  remains when the spectra are recorded in a thin cell at the perpendicular arrangement of the source and photoreceiver (see Fig. 3).

The dependence of the excitation and luminescence spectra on the optical path length at the frontal arrangement of the sample and a sharp change in the excitation

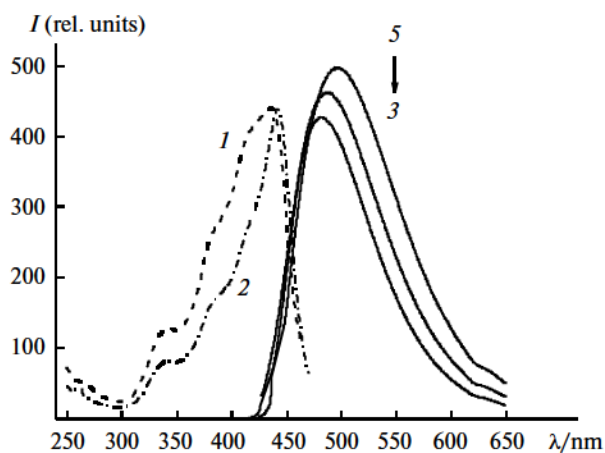


Fig. 5. Excitation spectra at  $\lambda_{\text{reg}} = 470$  (1) and 520 nm (2) and the luminescence spectra at  $\lambda_{\text{ex}} = 420$  (3), 430 (4), and 440 nm (5) of a solution of compound **1** in acetonitrile ( $C = 0.006 \text{ mol L}^{-1}$ ) at the frontal arrangement of the cell (1 mm thick).

spectra when the spectrum is recorded in a thin cell at the perpendicular arrangement, as well as the dependence of the position of the luminescence spectra maximum and the efficiency of concentration quenching on the exciting wavelength, indicate that the concentrated solution contains the second luminescence center caused by a weak dissociation of the molecules. The dependence of the excitation spectra on the registration wavelength proves that there are two luminescence centers in a saturated solution of compound **1** (see Figs 3 and 5). Indeed, as shown previously for a dilute solution ( $C = 10^{-5} \text{ mol L}^{-1}$ ), the excitation spectra nearly coincides with the absorption spectrum. However, as can be seen from Fig. 3, the low-intensity bands related to the excitation of monomeric luminescence and corresponding to the absorption spectrum remain in the short-wavelength region of the excitation spectrum of a concentrated solution of compound **1** at the same registration wavelength (470 nm). A new narrow band appears simultaneously in the excitation spectrum at  $\lambda_{\text{max}} = 450 \text{ nm}$ . The intense green luminescence with a maximum at 520 nm is observed upon excitation with  $\lambda_{\text{ex}} = 450 \text{ nm}$ . When the excitation spectrum is recorded at a wavelength of 520 nm, the bands corresponding to the absorption spectrum disappear from the spectrum and only a narrow band ( $\lambda_{\text{max}} = 450 \text{ nm}$ ) is observed (see Fig. 3). Only weak luminescence with the band maximum at 470 nm related to the luminescence of single molecules is detected for a concentrated solution of compound **1** upon excitation with  $\lambda_{\text{ex}} = 370 \text{ nm}$  (absorption band maximum). The lifetime of the excited state (for laser excitation with  $\lambda_{\text{ex}} = 370 \text{ nm}$ ) is approximated by one exponential curve being 0.95 ns, which is characteristic of the monomeric luminescence of compound **1**. The ratio of luminescence intensities at different exciting wavelengths is  $I_{450} : I_{370} \sim 15$ .

It should be emphasized that the possibility of observing the monomeric luminescence spectrum in a concentrated solution at the perpendicular arrangement of the cell and the difference in excitation spectra at different registration wavelengths show that the bathochromic shift of the luminescence maximum cannot be attributed only to self-absorption of compound **1** in a concentrated solution. The increase in the luminescence intensity with a change in the excitation wavelength from 370 to 450 nm indicates the formation of brightly luminescing associates in the solution. The excitation spectrum of these associates lies at the edge of the absorption spectrum of the luminophore in the region with a low absorbance. Since there are no differences in the spectral luminescence properties of the concentrated solution in a thin layer between the glasses and a dilute solution, it can be concluded that the concentration of the associates in solution is low. The number of the associates in the path of the light beam increases with an increase in the cell thickness, resulting in changes in the excitation and luminescence spectra (see Fig. 5).

**Table 3.** Shift of the position of the luminescence maximum ( $\lambda_{\max}$ ) at different exciting wavelengths ( $\lambda_{\text{ex}}$ ) under different conditions of spectra recording

$\lambda_{\text{ex}}/\text{nm}$	$\lambda_{\max}/\text{nm}$		
	I <sup>a</sup>	II <sup>b</sup>	III <sup>c</sup>
380	470	—	466
400	481	—	468
420	483	480	—
430	486	486	—
440	483	495	—
450	520	505	—

<sup>a</sup> I is the perpendicular arrangement of the cell.

<sup>b</sup> II is the frontal arrangement of the cell.

<sup>c</sup> III indicates a solution between the glasses at the frontal arrangement of the sample.

The observed pattern is probably similar to the "Weber red-edge effect," the essence of which is the bathochromic shift of the luminescence maximum and a decrease in the luminescence depolarization upon low-frequency excitation. The Weber effect is associated with the excitation of "long-wavelength" luminescence centers, whose number of small because of the fluctuation character.<sup>29,30</sup> The "long-wavelength centers" are formed due to the excitation of a considerable number of molecules in the charge-transfer state.<sup>31–34</sup> Note that the intense band in the excitation spectra of a concentrated solution of compound **1** lies at the long-wavelength edge of the absorption spectrum (see Fig. 3). The bathochromic shift of the luminescence maximum is observed with a gradual increase in the excitation wavelength (see Fig. 5, Table 3). No shift of the luminescence maximum is observed for recording of luminescence spectra of a solution of compound **1** between the glasses. Thus, by analogy to the published data,<sup>30–33</sup> the green luminescence ( $\lambda_{\max} = 520$  nm) in a concentrated solution of compound **1** can be assigned to the transition of a significant number of molecules **1** to the charge-transfer state and to the photoinduced formation of aggregates.

The further bathochromic shift of the excitation and luminescence maxima occurs on going from a saturated solution to crystals (Fig. 6). The excitation spectra of the crystals contains one intense band with a maximum at 470 nm bathochromically shifted relatively to the excitation band of aggregates in solution. Thus, the excitation of the aggregates occurs mainly in both crystals of compound **1** and its concentrated solution. Indeed, the crystal structure of stacks of compound **1** corresponds to the structure of J-aggregates of the "pack of cards" type<sup>24</sup> consisting of dimers (in this case, the dimer consists of two molecules between which an overlap of the phenyl and  $\beta$ -diketonate rings is observed (see Fig. 1, b)).

For crystals of compound **1**, as for concentrated solution, the excitation spectra maximum corresponds to the

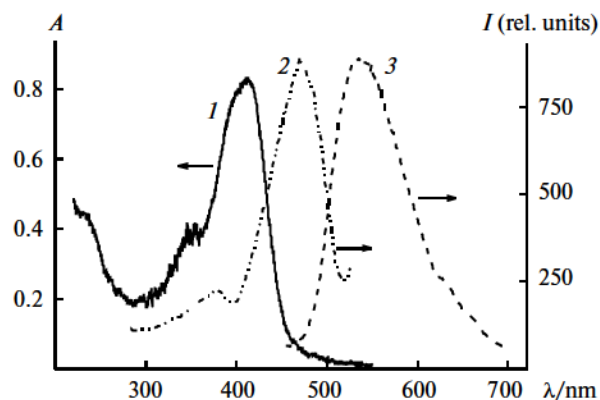


**Fig. 6.** Absorption (1), excitation (2), and luminescence (3) spectra of crystals of compound **1**.

long-wavelength edge of the absorption spectrum (see Fig. 7). However, unlike concentrated solutions, for crystals no dependence of the luminescence spectra on the excitation wavelength is observed. The luminescence decay kinetics of the crystal of compound **1** is approximated by three exponential curves, and the contribution of the exponents depends on the wavelength of luminescence registration ( $\lambda_{\text{reg}}$ ): at  $\lambda_{\text{reg}} = 470$  nm  $\tau_1 = 1.32$  ns (32.99%),  $\tau_2 = 2.82$  ns (49.18%), and  $\tau_3 = 16.80$  ns (17.83%); at  $\lambda_{\text{reg}} = 530$  nm  $\tau_1 = 1.24$  ns (5.25%),  $\tau_2 = 5.14$  ns (51.26%),  $\tau_3 = 12.79$  ns (43.49%). A significant contribution of the component with the shortest lifetime related to the luminescence of single molecule is observed at  $\lambda_{\text{reg}} = 470$  nm. An increase in the wavelength of luminescence registration (530 nm) increases the contribution of the component with the longest lifetime related to the luminescence of the excimers. In fact, the transient luminescence spectra of crystals (Fig. 7) show that two bands at 470 and 530 nm are observed in the luminescence spectra at the initial moment, and then the short-wavelength band disappears and the long-wavelength band undergoes a bathochromic shift

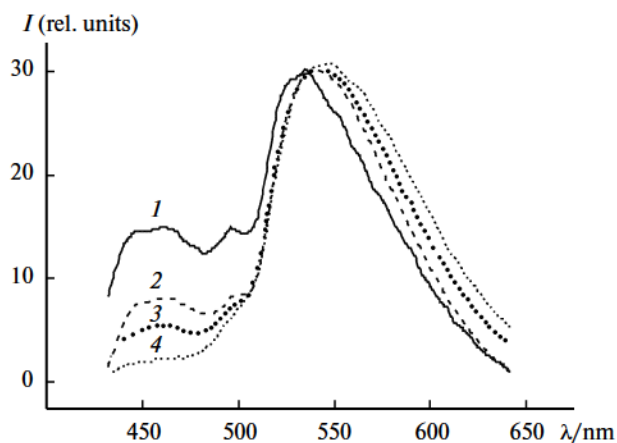


**Fig. 7.** Time-resolved luminescence spectra of crystals **1** 0 (1), 0.6 (2), 1.9 (3), and 5 ns (4) after laser pulse excitation.

by 15 nm. Thus, the laser excitation of the crystal ( $\lambda_{\text{ex}} = 370$  nm) results in the excitation of single molecules at the initial moment ( $\lambda_{\text{max}} = 470$  nm), and then excimers are formed ( $\lambda_{\text{max}} = 535$  nm). The crystal structure of compound **1** is favorable for excimer formation (see Fig. 1, *b*): the interplanar spacing is 3.5–3.7 Å and the  $\pi$ -systems of the interacting molecules are overlapped.<sup>35</sup> Therefore, in saturated solutions of compound **1** in acetonitrile, the excitation with the light with the wavelength corresponding to the excitation of single molecules results in monomeric luminescence. Unlike this, a similar excitation of crystals of compound **1** results in excimer luminescence.

Thus, we found that the photoinduced formation of aggregates is observed in concentrated solutions of compound **1**. A peculiarity of the crystal structure of compound **1** is presented by two directions of  $\pi$ -stacking interactions: the  $\pi$ - $\pi$ -interaction of the dibenzoylmethanate moieties of the molecules is observed *via* axis *a*, whereas the benzoyl groups undergo the  $\pi$ - $\pi$ -interaction *via* axis *c*. The stack structure corresponds to the structure of J-aggregates of the staircase type consisting of dimers. Two routes of excimer formation in crystal were revealed by steady-state and time-resolved spectroscopy: by the excitation of single molecules and by the excitation of aggregates.

## References

1. G. T. Morgan, *J. Chem. Soc.*, 1924, **125**, 1963.
2. T. Liu, A. D. Chien, J. Lu, G. Zhang, C. L. Fraser, *J. Mater. Chem.*, 2011, **21**, 8401.
3. M. J. Mayoral, P. Ovejero, M. Cano, G. Orellana, *Dalton Trans.*, 2011, **40**, 377.
4. H. Zhang, X. Hu, W. Dou, W. Liu, *J. Fluor. Chem.*, 2010, **131**, 883.
5. Ger (East) DD/-265266, 1987; *Chem. Abstr.*, 1990, **112**, 45278.
6. German patent 10152938; *Chem. Abstr.*, 2003, **123**, 378622.
7. T. E. Goliber, J. H. Perlstein, *J. Chem. Phys.* 1984, **80**, 4162.
8. G. Tamulaitis, V. Gulbina, A. Undzenas, L. Valkunas, *J. Lumin.*, 1999, **82**, 327.
9. R. Kammler, G. Bourhill, Y. Jin, C. Bräuchle, G. Görlitz, H. Hartmann, *J. Chem. Soc., Faraday Trans.*, 1996, **92**, 945.
10. WO 02/065600. *Chem. Abstr.*, 2003, **137**, 187010.
11. A. G. Mirochnik, B. V. Bukvetskii, E. V. Gukhman, V. E. Karasev, *J. Fluor.*, 2003, **13**, 157.
12. B. V. Bukvetskii, E. V. Fedorenko, A. G. Mirochnik, A. Yu. Beloliptsev, *Russ. J. Struct. Chem. (Engl. Transl.)*, 2012, **53**, 73 [*Zh. Strukt. Khim.*, 2012, **53**, 78].
13. A. G. Mirochnik, B. V. Bukvetskii, E. V. Gukhman, P. A. Zhikhareva, V. E. Karasev, *Russ. Chem. Bull. (Int. Ed.)*, 2001, **50**, 1612 [*Izv. Akad. Nauk, Ser. Khim.*, 2001, 1535].
14. A. Sakai, M. Tanaka, E. Ohta, Y. Yoshimoto, K. Mizuno, H. Ikeda, *Tetrahedron Lett.*, 2012, **53**, 4138.
15. Y. L. Chow, X. Cheng, C. I. Johansson, *J. Photochem. Photobiol. A: Chem.*, 1991, **57**, 247.
16. A. G. Mirochnik, E. V. Gukhman, P. A. Zhikhareva, V. E. Karasev, *Spectrosc. Lett.*, 2002, **35**, 309.
17. A. G. Mirochnik, E. V. Fedorenko, D. Kh. Shlyk, *Russ. J. Phys. Chem. (Engl. Transl.)* 2007, **81**, 1880 [*Zh. Fiz. Khim.*, 2007, **81**, 2096].
18. *Organic syntheses an annual publication of satisfactory methods for the preparations of organic chemicals*, Annual volumes 26–32, New York–London.
19. Bruker (1998), *SMART and SAINT-Plus. Versions 5.0. Data Collection and Processing Software for the SMART System*. Bruker AXS Inc., Madison, Wisconsin, USA.
20. G. M. Sheldrick, *SHELXTL/PC, Version 5/10, An Integrated System for Solving, Refining and Displaying Crystal Structures From Diffraction Data*, Bruker AXS Inc., Madison, Wisconsin, USA.
21. A. G. Mirochnik, B. V. Bukvetskii, E. V. Gukhman, P. A. Zhikhareva, V. E. Karasev, *Russ. Chem. Bull. (Int. Ed.)*, 2002, **51**, 1715 [*Izv. Akad. Nauk, Ser. Khim.*, 2002, 1574].
22. A. G. Mirochnik, B. V. Bukvetskii, E. V. Fedorenko, V. E. Karasev, *Russ. Chem. Bull. (Int. Ed.)*, 2004, **53**, 291 [*Izv. Akad. Nauk, Ser. Khim.*, 2004, 1].
23. P. Pringsheim, *Fluorescence and Phosphorescence*, New York – London, 1949.
24. B. I. Shapiro, *Russ. Chem. Rev.*, 2006, **75**, 433.
25. V. V. Serra, S. M. Andrade, M. G. P. M. S. Neves, J. A. S. Cavaleiro, S. M. B. Costa, *New J. Chem.*, 2010, **34**, 2757.
26. S. Kirstein, S. Daehne, *Int. J. Photoenergy*, 2006, ID 20363, 1.
27. L. V. Levshin, E. Yu. Bekhli, T. D. Slavinova, V. I. Yuzhakova, *Opt. Spekt. [Optics and Spectroscopy]*, 1974, **36**, 503 (in Russian).
28. N. L. Vekshin, *Zh. Prikl. Spektrosk.*, 1988, **49**, 31 [*J. Appl. Spectr. (Engl. Transl.)*, 1988, **49**].
29. L. V. Levshin, A. M. Saletskii, *Lyuminesentsiya i ee izmereniya: Molekulyarnaya lyuminesentsiya [Luminescence and Its Measurements: Molecular Luminescence]*, Izd-vo Mos. Gos. Univ., Moscow, 1989, 272 pp. (in Russian).
30. G. Weber, *Biochem. J.*, 1960, **75**, 137.
31. M. Aleksiejew, J. Heldt, J. R. Heldt, *J. Lumines.*, 2008, **128**, 1307.
32. A. P. Demchenko, A. I. Sytnik, *Proc. Nat. Acad. Sci. USA*, 1991, **88**, 9311.
33. M. Viard, J. Gallay, M. Vincent, O. Meyer, B. Robert, M. Paternostre, *Biophys. J.*, 1997, **73**, 2221.
34. V. I. Tomin, M. Brozis, J. Heldt, *Z. Naturforsch., Teil B*, 2003, **58a**, 109.
35. N. N. Barashkov, T. V. Sakhno, R. N. Nurmukhametov, O. A. Khakhel', *Russ. Chem. Rev.*, 1993, **62**, 539.

Received February 15, 2013;  
in revised form May 14, 2013